A rainfall-manipulation experiment with 517 *Arabidopsis thaliana* accessions

Moises Exposito-Alonso[1], Rocío Gómez Rodríguez[2], Cristina Barragán[1], Giovanna Capovilla[1], Eunyoung Chae[1], Jane Devos[1], Ezgi S. Dogan[1], Claudia Friedemann[1], Caspar Gross[1], Patricia Lang[1], Derek Lundberg[1], Vera Middendorf[1], Jorge Kageyama[1], Talia Karasov[1], Sonja Kersten[1], Sebastian Petersen[1], Leily Rabbani[1], Julian Regalado[1], Lukas Reinelt[1], Beth Rowan[1], Danelle K. Seymour[1], Efthymia Symeonidi[1], Rebecca Schwab[1], Diep Thi Ngoc Tran[1], Kavita Venkataramani[1], Anna-Lena Van de Weyer[1], François Vasseur[1], George Wang[1], Ronja Wedegärtner[1], Frank Weiss[1], Rui Wu[1], Wanyan Xi[1], Maricris Zaidem[1], Wangsheng Zhu[1], Fernando García-Arenal[2], Hernán A. Burbano[1], Oliver Bossdorf[3], Detlef Weigel[1]*.

[1] Department of Molecular Biology, Max Planck Institute for Developmental Biology, Tübingen, Germany

[2] Center for Plant Biotechnology and Genomics, Technical University of Madrid, Pozuelo de Alarcón, Spain

[3] Institute of Ecology and Evolution, University of Tübingen, Tübingen, Germany

*correspondence to: weigel@weigelworld.org

Running title: A Climate Change Experiment with *A. thaliana*

The gold standard for studying natural selection and adaptation in the wild is to quantify lifetime fitness of individuals from natural populations that have been grown together in a common garden, or that have been reciprocally transplanted. By combining fitness values with species traits and genome sequences, one can infer selection coefficients at the genetic level. Here we present a rainfall-manipulation experiment with 517 whole-genome sequenced natural accessions of the plant *Arabidopsis thaliana* spanning the global distribution of the species. The experiments were conducted in two field stations in contrasting climates, in the Mediterranean and in Central Europe, where we built rainout shelters and simulated high and low rainfall. Using custom image analysis we quantified fitness- and phenology-related traits for 23,154 pots, which contained about 14,500 plants growing independently, and over 310,000 plants growing in small populations (max. 30 plants). This large field experiment dataset, which associates fitness and ecologically-relevant traits with genomes, will provide an important resource to test eco-evolutionary genetic theories and to understand the potential evolutionary impacts of future climates on an important plant model species.

Background and Summary

Darwin's theory of evolution by natural selection states that when individuals of a population have distinct traits that improve their ability to survive and reproduce, and these are heritable, the population will change and adapt over generations[1]. This was formally described by R. A. Fisher[2], stating that the higher the genetic variance in fitness, the higher the rate of adaptation of a species. Natural selection over morphological, physiological or other traits has been studied in a wide range of organisms[3–6] using observational and experimental fitness measurements of multiple individuals in field conditions. However, studies that combine such measurements with knowledge on genome-wide variation are, in comparison, very rare[7–9]. This is surprising, given that they can enable the translation of selection coefficients to the genetic level and thus ultimately help us to understand whether traits will evolve over generations.

With climate change, the study of adaptation to the environment has acquired new importance. Predictions of climate change indicate not only that temperature will rise, but that also precipitation regimes will be altered, leading to more frequent and extreme droughts[10], posing the critical question of whether populations will be able to adapt or will become extinct[11]. Field experiments where climate variables such as rainfall are manipulated can be used to address this question[12].

Here we present a high-throughput field experiment with 517 whole-genome sequenced natural lines of *Arabidopsis thaliana*[13] grown under rainfall-manipulation conditions at two field stations with contrasting

2

climate. This experiment was designed to be of a sufficiently large scale to enable powerful genome-wide association analyses[14] and to maximize the replicability of species-wide patterns, which increases with the diversity of genotypes included in an experiment[15]. This dataset will be invaluable for the study of natural selection and adaptation in the context of global climate change at the genetic level[16], building on the genetic catalog of the 1001 Genomes Project[13] and complementing the already published extensive set of traits measured in controlled growth chamber or greenhouse conditions[17,18].

Methods

Accessions from the 1001 Genomes Project

The 1001 Genomes (1001G) Project[13] has provided information on 1,135 natural lines or accessions and 11,769,920 SNPs and small indels called after re-sequencing (Fig. 1). To select the most genetically and geographically informative 1001G lines, we applied several filters: (1) First we removed the accessions with the lowest genome quality. We discarded those with < 10X genome coverage of Illumina sequencing reads and < 90% congruence of SNPs called from MPI and GMI pipelines[13]. (2) We removed near-identical individuals. Using Plink[19] we computed identity by state across the 1,135 accessions. For pairs of accessions with < 0.01 differences per SNP (<100,000 variants approx.), we randomly selected one accession to include in our study. (3) Finally, we reduced geographic sampling ascertainment bias, as the sampling for 1001G was performed in neither a random nor a regularly structured scheme. Some laboratories provided several lines per location whereas others provided lines that were collected at least several hundred kilometres apart. Using each accession's collection location, we computed Euclidean distances across the 1,135 accessions and identified all pairs that were apart less than 0.0001 Euclidean distance in degrees latitude and longitude (<< 100 meters). From such pairs, we randomly selected one accession to remain. After applying criteria (1), (2), and (3), we obtained a final set of 523 accessions (Datasets 1 and 2). To bulk seeds for our rainfall-manipulation experiment and control for maternal effects, we first propagated accessions in controlled conditions. We stratified the seeds one week at 4°C, we sowed them in trays with industrial soil (CL-P, Einheitserde Werkverband e. V., Sinntal-Altengronau Germany) and placed them in a growth room with 16 h light and 23°C for one week. Trays were vernalized for 60 days at 4°C and 8h daylength. After vernalization, trays were moved back to 16 h light and 23°C for final growth and reproduction. This generated sufficient seeds for 517 accessions, which were later grown in the field in two locations (Fig. 1). Seeds originating from the same parents can be ordered from the 1001G seed stock at the Arabidopsis Biological Resource Center (CS78942).
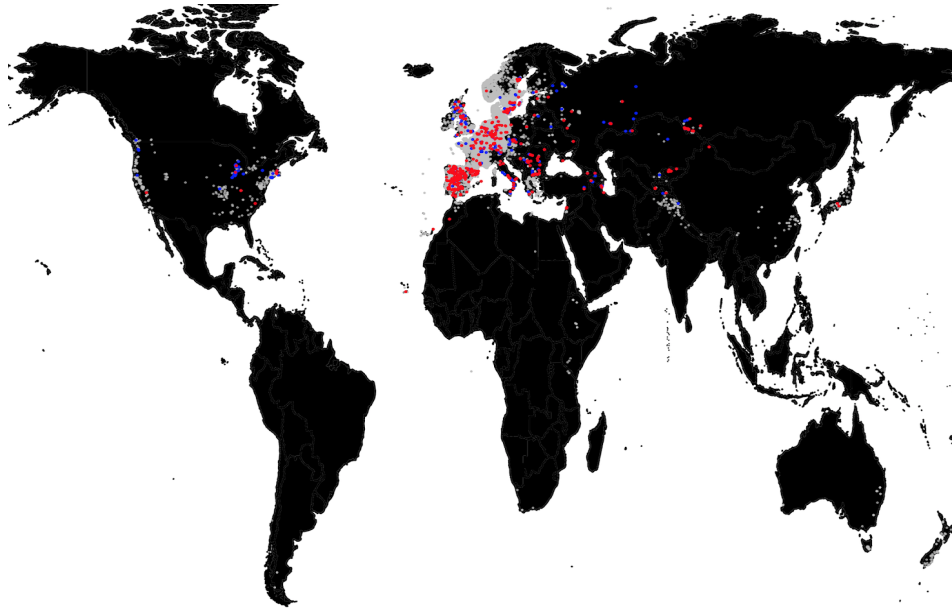
Figure 1. Geographic distribution of accessions. Locations of *Arabidopsis thaliana* accessions used in this experiment (red), 1001G accessions (blue), and all sightings of the species in gbif.org (grey).

Field experiment design

Rainout shelter design

We built two 30 m x 6 m tunnels of PVC plastic foil to fully exclude rainfall in Madrid (Spain, 40.40805ºN -3.83535ºE) and in Tübingen (Germany, 48.545809ºN 9.042449ºE) (Fig. 2). The foil tunnels are different from a regular greenhouse in that they are completely open on two sides. Thus, ambient temperatures vary virtually as much as outside the foil shelter (see Environmental sensors section). In each location, we supplied artificial watering in two contrasting regimes: abundant watering and reduced watering. Inside each tunnel, we created a 4% slope, and four flooding tables (1 m x 25 m, Hellmuth Bahrs GmbH & Co KG, Brüggen, Germany) covered with soaking mats (4 l/m^2, Gärtnereinkauf Münchingen GmbH, Münchingen, Germany) were placed on the ground in parallel to the slope. Water was able to drain at the lower end of the flooding table (Fig. 2). A watering gun was used to manually simulate rainfall from the top.

For sowing, we used potting trays with 8x5 cells (5.5 cm x 5.5 cm x 10 cm size) and industrial soil (CL-P, Einheitserde Werkverband e.V., Sinntal-Altengronau Germany). One genotype was sown per cell, excluding corner cells, to avoid extreme edge effects. We grew a total of 12 replicates per genotype per treatment: Five replicates were sown at high density, with 30 seeds per cell and without further intervention ("population replicate"). The remaining seven replicates were planted at low density (ca. 10 seeds) and one seedling was selected at random after germination ("individual replicate"). Excess individuals were culled. While the

population replicates should more faithfully reflect survival from seed to reproduction, the individual replicates were useful to more accurately monitor flowering time and seed set.

We used a randomized incomplete block design (Fig. 2). One block of the 517 genotypes spanned 14.36 trays (36 cells/tray), and genotypes were randomized within each block. The design was identical in Madrid and Tübingen (Fig. 2).
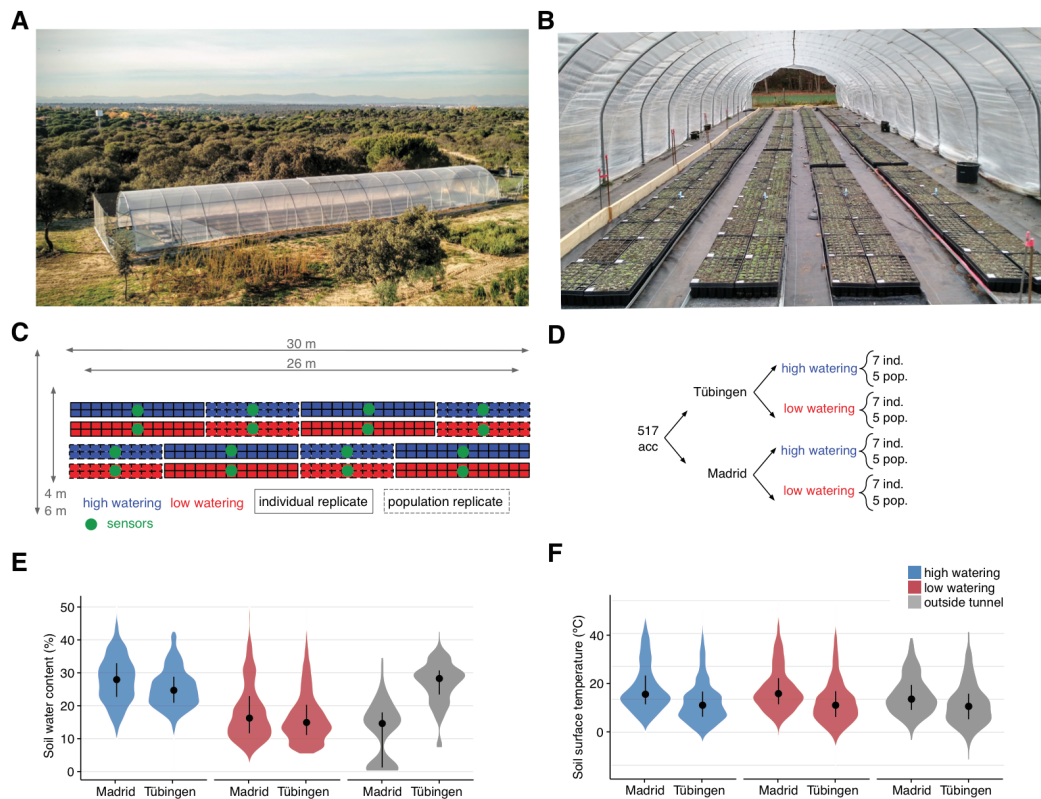
Figure 2. Field experiment design. (A) Aerial view of foil tunnel settings in Madrid and (B) view inside the foil tunnel in Tübingen. (C) Spatial distribution of blocks and replicates and (D) experimental design. (E) Soil water content and (F) soil surface temperature from the 34 sensors monitoring each experimental block and conditions outside the tunnel.

Environmental sensors

Environmental variables — air temperature, photosynthetically active radiation (PAR) and soil water content — were monitored every 15 minutes for the entire duration of the experiment using multi-purpose sensors (Flower Power, Parrot SA, Paris, France). This enabled us to adjust watering depending on the degree of local

evapotranspiration during the course the experiment. The sensors outside of the tunnel in Madrid (i.e. only natural rainfall) showed an interquartile range between 1% and 17% soil water content. This overlapped with the range of 10 to 22% water content of the drought treatment that we artificially imposed inside the tunnels in Madrid and Tübingen. The lower range of measurements in Madrid (outside sensor) is due to a lack of natural rainfall during the first two months of the experiment. In contrast, the sensor outside the tunnel in Tübingen recorded an interquartile range of soil water content percentage of 22 to 27%, which was comparable to the high watering treatments in Tübingen and Madrid (from 20 to 33%). These values confirmed that our low and high watering treatment were not only different, but also that they mimicked natural soil water content at the two contrasting locations. Mean daily air temperatures (measured by the sensors at 5-10 cm above the soil surface every 15 minutes) were overall higher in Madrid (8-10°C) than in Tübingen (5-6°C), and the difference in temperature between the sensors inside and outside the tunnels was in both locations on average only 1°C (Table 1). The photosynthetically active radiation (PAR, wavelengths from 400 to 700 nm) had a median of 0.1 mol m^{-2} day^{-1} at night for all experiments. At mid-day (11:00-13.00 hrs), the median PAR in Madrid was 57.8 mol m^{-2} day^{-1} outside, and 45.7 mol m^{-2} day^{-1} inside the tunnel. In Tübingen, the median values were 29.0 outside, and 30.9 mol m^{-2} day^{-1} inside the tunnel.

Table 1 Summaries of environmental sensor measurements

A total of 34 sensors were placed in the different treatment blocks (low/high) as well as outside (out) of the foil tunnels (Fig. 2). The median (interquartile) values of all sensors per treatment and location are shown.

Site	Rainfall	Soil water content (%)	Air temperature (ºC)
Madrid	out	14.5 (1.09, 17.46)	8.5 (5.34, 12.39)
Madrid	low	16.1 (11.38, 22.51)	10.0 (6.95, 15.13)
Tuebingen	low	14.7 (10.76, 20.09)	6.6 (3.27, 10.78)
Tuebingen	out	27.7 (22.82, 30.50)	5.6 (2.44, 9.54)
Tuebingen	high	24.6 (20.73, 29.02)	6.6 (3.27, 10.78)
Madrid	high	27.8 (22.62, 33.00)	9.8 (6.82, 15.13)

Sowing and quality control

During sowing, contamination of neighboring pots with adjacent genotypes can occur for multiple reasons. In order to avoid such contamination, we chose a day with no wind and sowed seeds at 1-2 cm height from the soil. Additionally, we took care during the first days to be particularly gentle when using the watering gun to avoid seed-carryover (bottom watering by flooding was done regularly). We also tried to remove human error during sowing by preparing and randomizing 2 ml plastic tubes containing the seeds to be sown in the same layouts (5x8) as the destination trays. During sowing, each experimenter took a box at random and went to the

160   corresponding labeled and arranged tray in the field (Fig. 2). This reduced the possibility of sowing errors.

161   During vegetative growth, we could identify seedlings that resembled their neighbors or were located in the

162   border between two pots and removed such plants as potential contaminants. We also used the homogeneity

163   of flowering within a pot in the population replicates as a further indicator for contamination. When a plant

164   had a completely different flowering timing or vegetative phenotypes did not coincide with the majority of

165   plants in the pot, this plant was removed. After sowing and quality control, the total number of pots was

166   24,747 instead of the original 24,816 pots (99.7%).

167   **Field monitoring**

168   Image analysis of vegetative rosettes

169   Top-view images were acquired every four to five days (median in both sites) with a Panasonic DMC-TZ61

170   digital camera and a customized closed dark box, the "Fotomatón" (Fig. 3), at a distance of 40 cm from each

171   tray. In total, we imaged each tray at 20 timepoints throughout vegetative growth. The implemented

172   segmentation was the same as in Exposito-Alonso et al. [20], which relies on the Open CV Python library[21]. We

173   began by transforming images from RGB to HSV channels. We applied a hard segmentation threshold of HSV

174   values as (H=30-65, S=65-255, V=20-220). The threshold was defined after manually screening 10 different

175   plants in order to capture the full spectrum of greens both of different accessions and of different

176   developmental stages. This was followed by several iterations of morphology transformations based on erosion

177   and dilation. For each of the resulting binary images we counted the number of green pixels.

178   During field monitoring, we noticed that some pots were empty because seeds had not germinated. In

179   these cases, we left a red marker in the corresponding pots, which could be detected in a similar way as the

180   presence of green pixels (with threshold H=150-179, S=100-255, V=100-255). These pots were excluded from

181   survival analysis as they did not contain any plants. An example of transformed images is shown in Fig. 3. The

182   resulting raw data consist of green and red pixel counts per pot (Fig. 3). In order to detect the red markers

183   automatically, we performed an analysis of variance between pots above and below a threshold of red pixels

184   and finding the threshold that maximized this separation. This provided us with the threshold of red pixels

185   above which a pot had a red marker (indicating an empty pot). As expected, the distribution of pixels was

186   bimodal, making this identification straightforward (Fig. 3C).

187   We estimated germination timing by analysing trajectories (Fig. 3) of green pixels per pot, and

188   identifying the first day that over 1,000 green pixels were observed in a pot (corresponding to a plant size of ~

189   10 mm^2, Fig. 4). The final dataset contained data for 22,779 pots — after the removal of pots with red labels —

190   with a time series of green pixel counts.
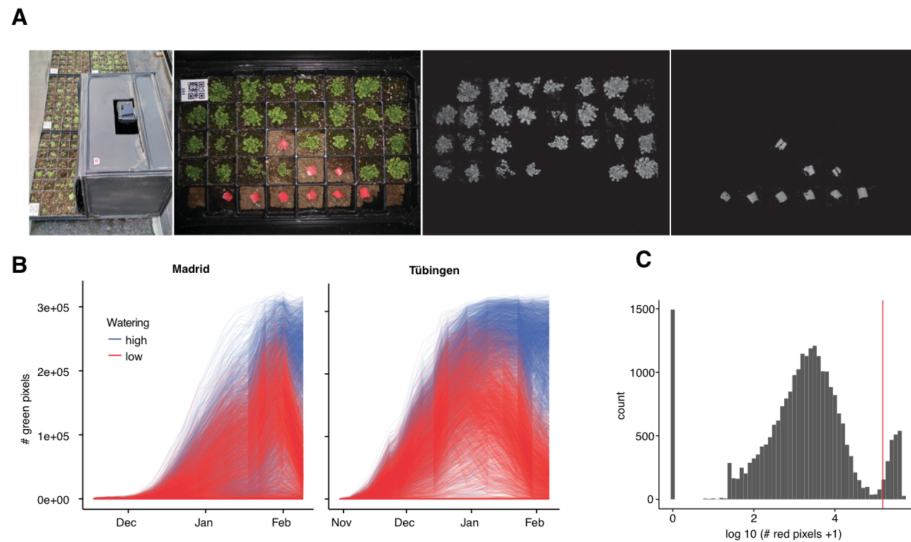
Figure 3. Rosette monitoring. (A) Customized dark box ("Fotomatón") for image acquisition and example tray with the corresponding green and red segmentation. (B) Trajectories of number of green pixels per pot, indicating rosette area, for Madrid and Tübingen. (C) Distribution of the sum of red pixels per pot over all time frames. The red vertical line indicates the heuristically chosen threshold to define whether the pot actually had a red marker.

Manual recording of flowering time

196   We visited the experimental sites every 1-2 days and manually recorded the pots with flowering plants.

197   Flowering time was measured as the day when the first white petals could be observed with the unaided eye.

198   This criterion was chosen as sufficiently objective to reduce experimenter error. To keep track of previous visits

199   and avoid errors, we labeled the pots where flowering had already been recorded with blue pins. To calculate

200   flowering time, we counted the number of days from the date of sowing to the recorded flowering date (we

201   did not use the inferred day of germination to avoid introducing modeling errors in the flowering time metric).

202   Fig. 4 shows the raw flowering time data per pot in the original spatial distribution (Fig. 2) and the distribution

203   of flowering time per treatment combination. Note that grey boxes in Fig. 4 are pots with plants that did not

204   survive until flowering. In total, we gathered data for 16,858 pots with flowering plants.
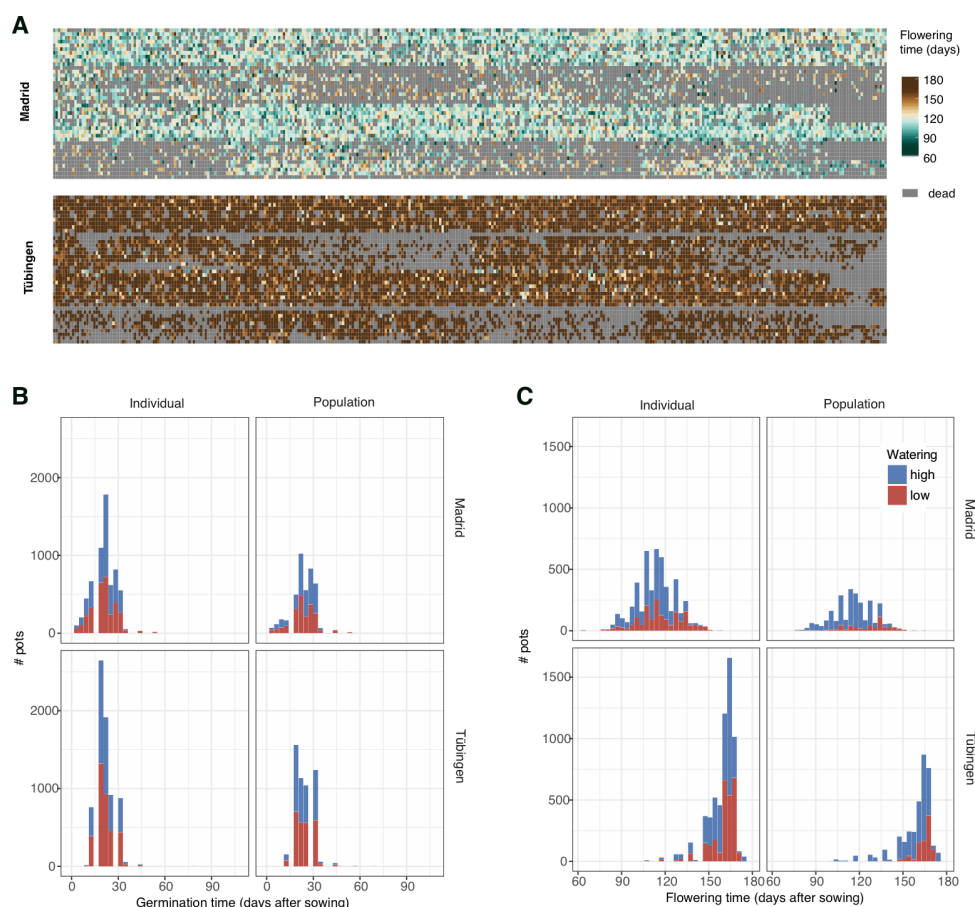
Figure 4. Flowering time distributions. (A) Flowering times per pot in the same spatial arrangement as in each tunnel (see Fig. 3). (B) Distribution of germination times. (C) Distribution of flowering times.

Image analysis of reproductive plants

Once the first dry fruits were observed, we harvested them and took a final 'studio photograph' of the rosette and the inflorescence (Fig. 5). In total, we took 13,849 photographs. The camera settings were the same as for the vegetative monitoring, but here we included an 18% grey card approximately in the same location for each picture in case *a posteriori* white balance adjustments would be needed. We first used a cycle of morphological transformations of erode-and-dilate to produce the segmented image (Fig. 5). This generated a segmented white/black image without white noise. Then, we used the thin (erode cycles) algorithm from the Mahotas Python library[22] to generate a binary picture reduced to single-pixel paths — a process called skeletonisation (Fig. 5). Finally, to detect the branching points in the skeletonised image we used a hit-or-miss algorithm. We used customized structural elements to maximize the branch and end point detection (Fig. 5). This resulted in four variables per image: total segmented inflorescence area, total length of the skeleton path, number of branching points, and number of end points (Fig. 5).
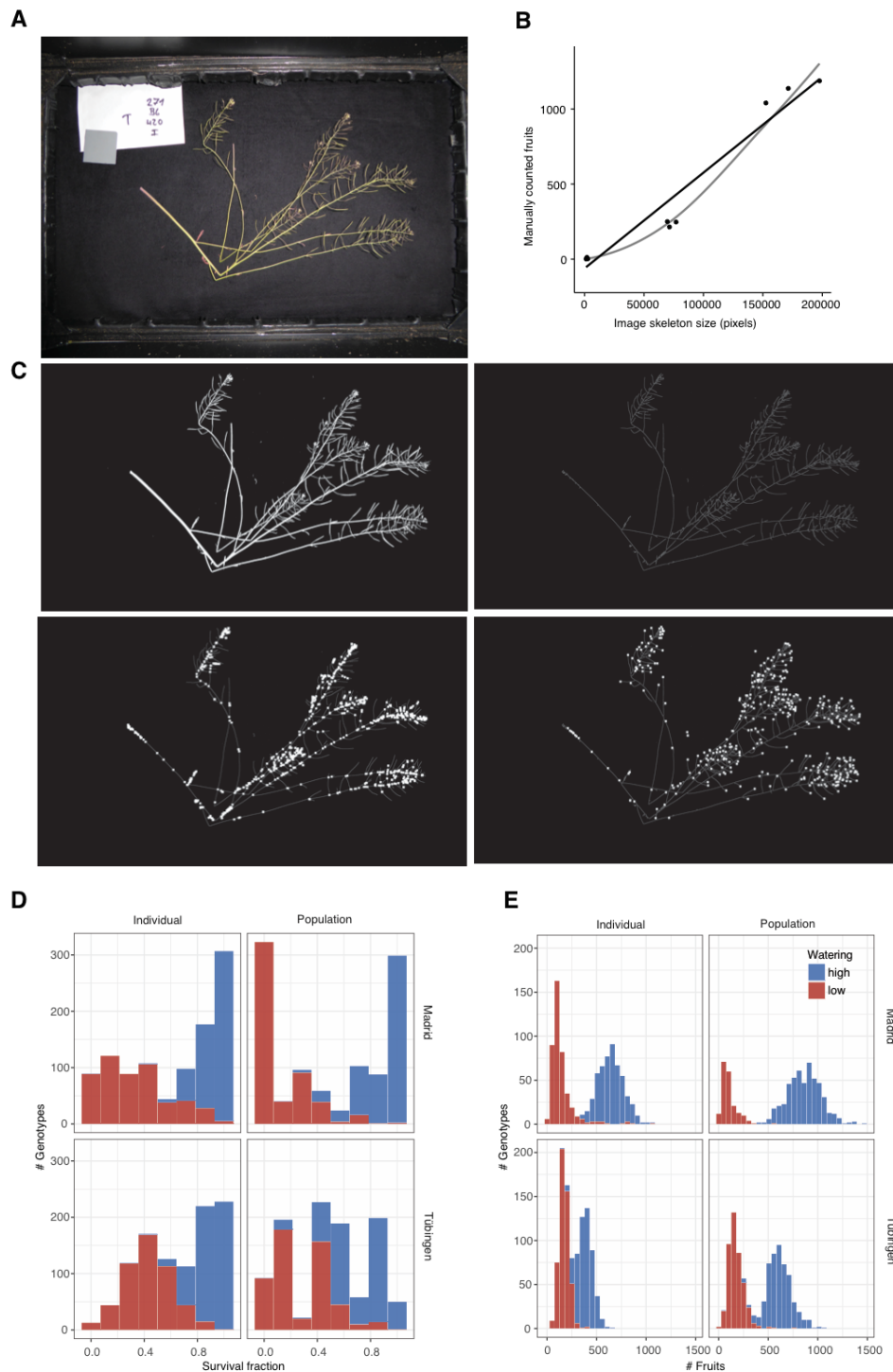
Figure 5. Inflorescence and seed set estimation. (A) Representative inflorescence picture. (B) Regression between the fruits of a few manually counted inflorescences and the inflorescence size calculated based on image processing. The four variables inferred in (C) accurately predicted the visually counted inflorescences as example (R^2=0.97, n=11, P=10^{-4}). (C) Resulting variables from image processing of (A): total segmented area (upper-left), skeletonized inflorescence (upper-right), branching points (lower-left), and endpoints (lower-right). Distribution of survival to reproduction (D) and fruits per plant (E) in the four environments.

225   <u>Estimation of fruit and seed number</u>

226   Although the study of natural selection is based on studying relative fitness, and total reproductive area might

227   provide a good relative estimate, sometimes it is useful to have a proxy of the absolute fitness. In order to

228   provide an approximate number of how many seeds each plant had produced, we generated two allometric

229   relationships by visual counting of fruits per plant and seeds per fruit. In order to be sure that the counts

230   corresponded to single plants, we counted fruits and seeds of only individual replicates of accessions, not the

231   population replicates (see Field experiment design section). Because a strong relationship had already been

232   validated between inflorescence size and the number of fruits in a number of studies with *A. thaliana*[23–25], we

233   decided that counting a few inflorescences of three sizes, reflecting the broad size spectrum, would be

234   sufficient to establish a first allometric relationship with the four image-acquired variables (n=11

235   inflorescences, R^2=0.97, *P*=4×10^{-4}, Fig.5B,C). To express fecundity as the number of seeds, we counted all

236   seeds inside one fruit for each of the inflorescences used for the first allometric relationship (n=11 fruits),

237   aiming for a wide range of fruit sizes. The mean was 28.3 seeds per fruit and the standard deviation was 11.2

238   seeds. The two aforementioned allometric relationships were used to predict, first, the number of fruits per

239   inflorescence using the four image analysis variables, and second, the number of seeds corresponding to the

240   number of fruits per inflorescence.

241   **Data records**

242   The main datasets of accession information and trait values measured in the field for all replicates as well as

243   curated averages per genotype are available as supplementary information at xxx. The datasets are also part of

244   the R package "dryAR" available at http://github.com/MoisesExpositoAlonso/dryAR with doi xxx.

245   **Table 2 Variable descriptions**

246   Variable names and their descriptions and units are reported. All datasets share a common accession identification

247   number.

Dataset	Variable	Information
D1&D2&D3&D4	id	Unique numeric ID assigned to the accessions included in the 1001 Genomes Project
D1&D2	name	Classic accession name assigned by original collector
D1&D2	country	Country of collection
D1&D2	sitename	Toponym of the location of collection
D1&D2	latitude	Degrees North of the location of origin (°N)
D1&D2	longitude	Degrees East of the location of origin (°E)
D1&D2	collector	Original researcher that collected the accession
D1&D2	collectiondate	Calendar date of collection
D1&D2	CS_number	Stock number in the Arabidopsis Biological Resource Center (abrc.osu.edu)
D1&D2	Q_SNPcongruency	Pass/no pass of thresholds for genome quality and SNP calling congruency
D1&D2	Q_geneticsdist	Pass/no pass of the filter for almost identical accessions

D1&D2	Q_geodist	Pass/no pass of filter for geographically close accessions
D1&D2	is_relict	Belongs to the Mediterranean "relict" lineage
D1&D2	finalset	Included in the final 517 set for the field experiment
D3&D4	site	Field station site. m=Madrid(Spain), t=Tübingen(Germany)
D3&D4	water	Rainfall/watering treatment. h=high rainfall, l=low rainfall
D3&D4	indpop	Density of plants per pot. i=single plant selected after germination, p=population of 30 seeds growing undisturbed
D3&D4	qpblock	Identification number of quickpot (tray) within treatment block (rainfall row x replicate block) (see Fig. 2)
D3&D4	qp	Identification number of quickpot tray in the whole experiment
D3&D4	qp_x	Pot position in x axis within the quickpot tray
D3&D4	qp_y	Pot position in y axis within the quickpot tray
D3&D4	pos	Pot x,y coordinate within the quickpot tray
D3&D4	rep	Replicate number
D3&D4	trayid	Identification of the tray combining block and treatments
D3&D4	potindex	Identification of pot combining site, tray, and position within the tray
D3&D4	Germination_time	Inference of germination time based on the day that rosette area was over 1,000 pixels size (days after sowing)
D3&D4	Green	Sum of all green areas per pot throughout the experiment (# pixels). This helps to identify successfully growing pots.
D3&D4	Red	Sum of all red areas per pot throughout the experiment (# pixels). This helps to identify red tags placed on pots that failed throughout the experiment
D3&D4	Survival_flowering	Survival until reproduction (i.e. production of flowers)
D3&D4	Flowering_date	Date that the first flowers had developed
D3&D4	Flowering_time	Time from sowing until the date of flowering (days)
D3&D4	Inflorescence_size	Area of inflorescence (#pixels)
D3&D4	Survival_num	Number of surviving plants until fruit set. Only applies to "population" pots.
D3&D4	Survival_fruit	Survival until fruit set (i.e. produced fruits)
D3&D4	Fruits	Number of fruits inferred from the function between visually counted fruits and inflorescence area, total path, branching points, and ending points.
D3&D4	Seeds	Number of seeds inferred from the average number of seeds per fruit and number of fruits.
D3&D4	Infloresncence_byind	Area of inflorescence (#pixels) divided by total number of plants per pot. Only applies to "population" pots.
D3&D4	Fruits_byind	Number of fruits divided by total number of plants per pot. Only applies to "population" pots.
D3&D4	Seeds_byind	Number of seeds divided by total number of plants per pot. Only applies to "population" pots.
D3&D4	Fitness	Lifetime fitness (number of seeds / seed planted). This metric integrates survivorship and reproduction.

Technical validation

Data processing

All images are deposited at [updatehere]. The Python modules to process images for green area segmentation and inflorescence analyses are available at http://github.com/MoisesExpositoAlonso/hippo and http://github.com/MoisesExpositoAlonso/hitfruit, along with example datasets.

389   To reproduce our data curation procedure we created the R package dryAR
390   (http://github.com/MoisesExpositoAlonso/dryAR with doi xxx). All scripts to re-generate data from raw files
391   can be found at http://github.com/MoisesExpositoAlonso/dryAR/data-cleaning.

392   *Replicability of image processing*

393   After testing different camera parameters, we used an exposure of -2/3 and an ISO of 100. White balance was

394   set for flashlight. We used a dark box with all sides closed, so the flashlight was the only source of illumination.

395   This ensured that the white balance and illumination were virtually consistent from picture to picture, as

396   shown before[20]. Photos were saved both in .jpeg and .raw to allow for *a posteriori* adjustments if needed.

397   Using a calibration board with 1.3 cm x 1.3 cm white and dark squares, we examined the error between the

398   inferred area from image analysis and the real 1.3 cm-side squares across the tray. This provided us with a

399   median resolution estimate of 101.5 pixels mm^{-2}. The deviations from the true area were minimal, with a

400   median of 2.7% and values of 1.4% / 4.2% for the 1st and 3rd quartile. The maximum area deviations were of 8

401   to 9% in the extreme corners of the tray, where we did not sow any seeds. We are confident that such small

402   variation in retrieved area is compensated by the randomized locations of genotypes within the trays.

403   To further verify that our camera settings and segmentation pipeline produced replicable extractions of

404   plant green area, we used images of trays that were photographed twice on the same day by mistake. In total

405   there were 1,508 such pots distributed across 11 timepoints and different trays. By comparing the area of the

406   same pot of two different camera shots and segmentation analyses, we could verify that the Spearman's rank

407   correlation was very high (r=0.97, n=1508, *P*<10^{-16}), confirming high replicability.

408   Because we ran the same segmentation and skeletonization software on both rosette and

409   inflorescence images, we could leverage the clearly different image patterns that rosettes and inflorescences

410   have to identify labeling errors (i.e. mistakes in manually inputting sample information of the pictures). To do

411   this, we first trained a random forest model to predict the manually labeled "rosette" or "inflorescence" by the

412   four image variables in Fig. 5. By fitting a Random Forest with all images, we find that the leave-one-out

413   accuracy was 92.1%, i.e. ca. 2,000 images were incorrectly labeled by the algorithm. We manually checked

414   whether these were mislabeled or rather whether they "looked similar" in terms of area or landmark points in

415   the photo, e.g. when both rosette or inflorescences were diminute. We found that only 2.5% were incorrectly

416   mislabeled (and corrected them) and are thus confident that the labeling error must be below 2.5%.

417   *Experimental validation*

13

418   Although repeating experiments in climatically-similar locations would be impractical, we could verify that

419   survival in Madrid and low precipitation correlated with a preliminary drought experiment in the greenhouse

420   (Spearman's rho=0.17, n=211, *P*=0.01)[20]. On the other hand, reproductive allocation measured under optimal

421   conditions in the greenhouse correlated with total seed output in the most similar field experiments, Tübingen

422   high precipitation (Spearman's rho=0.27, n=211, *P*=5x10^{-5})[23].

423   **ADDITIONAL INFORMATION**

424   **Acknowledgements**

428   **Supplementary Information** accompanies this paper at xxx

429   **Competing interests**: The authors declare no competing financial interests.

432   **Author contributions**

433   MEA conceived and designed the project. MEA carried out the experiment in Tübingen. MEA and RGR carried

434   out the experiment in Madrid. All authors contributed to specific tasks in the experiments (see detailed

435   description below). OB provided the field site in Tübingen and FGA provided the site in Madrid. DW secured

436   funding for the project. MEA carried out the analyses and wrote the first draft of the manuscript. All authors

437   edited, commented and approved the manuscript.

AUTHOR	Conceived_idea	Funding	Advice	Coordination	Materials	Bulking_seeds	Seed_aliquoting	Field_setup	Pictures_plants	Sowing_Madrid	Sowing_Tuebingen	Thinning_seedlings	Field_care	Image_processing	Foil_tunnel_reparation	Fresh_harvesting_Madrid	Fresh_harvesting_Tuebingen	Dry_imaging_Madrid	Dry_imaging_Tuebingen	Flowering_monitoring	Image_processing	Data analysis/processing	Writing
Moises Exposito-Alonso	x			x	x	x	x	x	x	x	x	x	x	x	x	x	x	x	x	x	x	x	x
Rocio Gomez Rodriguez							x	x	x	x			x			x				x			
Detlef Weigel		x	x	x													x						
Hernán A Burbano			x						x														
Oliver Bossdorf			x		x																		
Rebecca Schwab			x	x	x												x						
Fernando García Arenal			x		x																		
George Wang			x																				
François Vasseur			x								x												
Julian Regalado							x																
Derek Lundberg											x						x						
Ronja Wedegärtner							x	x	x		x		x				x						
Frank Weiss									x														
Danelle Seymour											x												
Beth Rowan											x				x		x						
Patricia Lang									x		x	x			x	x	x						
Jorge Kagayema											x												
Rui Wu											x				x		x						
Wanyan Xi											x												
Kavita Venkataramani											x				x	x	x						
Giovanna Capovilla												x			x		x						
Efthymia Symeonidi									x			x			x		x						
Vera Middendorf												x							x	x			
Anna-Lena Van de Weyer												x											
Jane Devos												x											
Diep Thi Ngoc Tran												x											
Sonja Kersten					x						x				x								
Wangsheng Zhu															x								
Maricris Zaidem															x								
Sebastian Petersen																	x						
Ezgi Dogan																	x						
Claudia Friedemann																x	x						
Talia Karasov																	x						
Cristina Barragán																	x						
Leily Rabbani																	x						
Caspar Gross																	x					x	
Lukas Reinelt													x									x	
Eunyoung Chae																	x						

Datasets

438

439

Dataset 1 Quality-based selection of the original 1,135 accessions

440 We report the 1001 Genome identification numbers, the quality filters that each accession passed during the

441 selection of the 517 set.

442

Dataset 2 Description of the 517 accessions

443 We report the final set of 517 accessions that were used in the field experiment.

444

Dataset 3 All traits measured per replicate

445 For each pot replicate, we report all raw data as well as composite variables.

446

Dataset 4 Curated means per accession

447 For each accession, we report all data as well as composite variables.

REFERENCES

1. Darwin, C. *The Origin of Species*. (John Murray, 1859).

2. Fisher, S. R. A. *The genetical theory of natural selection*. (The Clarendon Press, 1930).

3. Hereford, J. A quantitative survey of local adaptation and fitness trade-offs. *Am. Nat.* **173,** 579–588 (2009).

4. Kingsolver, J. G. *et al.* The strength of phenotypic selection in natural populations. *Am. Nat.* **157,** 245–261 (2001).

5. Siepielski, A. M. *et al.* The spatial patterns of directional phenotypic selection. *Ecol. Lett.* **16,** 1382–1392 (2013).

6. Siepielski, A. M., DiBattista, J. D. & Carlson, S. M. It's about time: the temporal dynamics of phenotypic selection in the wild. *Ecol. Lett.* **12,** 1261–1276 (2009).

7. Thurman, T. J. & Barrett, R. D. H. The genetic consequences of selection in natural populations. *Mol. Ecol.* **25,** 1429–1448 (2016).

8. Gompert, Z. *et al.* Experimental evidence for ecological selection on genome variation in the wild. *Ecol. Lett.* **17,** 369–379 (2014).

9. Anderson, J. T., Lee, C.-R. & Mitchell-Olds, T. Strong selection genome-wide enhances fitness trade-offs across environments and episodes of selection. *Evolution* **68,** 16–31 (2014).

10. Dai, A. Increasing drought under global warming in observations and models. *Nat. Clim. Chang.* **3,** 52–58 (2012).

11. Hoffmann, A. A. & Sgrò, C. M. Climate change and evolutionary adaptation. *Nature* **470,** 479–485 (2011).

12. Tielbörger, K. *et al.* Middle-Eastern plant communities tolerate 9 years of drought in a multi-site climate manipulation experiment. *Nat. Commun.* **5,** 5102 (2014).

13. 1001 Genomes Consortium. 1,135 Genomes Reveal the Global Pattern of Polymorphism in Arabidopsis thaliana. *Cell* **166,** 481–491 (2016).

14. Burghardt, L. T., Young, N. D. & Tiffin, P. A Guide to Genome-Wide Association Mapping in Plants. *Current*

16

   Protocols in Plant Biology 22–38 (2017).

15. Milcu, A. *et al.* Genotypic variability enhances the reproducibility of an ecological study. *Nat Ecol Evol* **2,** 279–287 (2018).

16. Exposito-Alonso, M., Burbano, H. A., Bossdorf, O., Nielsen, R. & Weigel, D. A map of climate change-driven natural selection in Arabidopsis thaliana. *bioRxiv* 321133 (2018). doi:10.1101/321133

17. Seren, Ü. *et al.* AraPheno: a public database for Arabidopsis thaliana phenotypes. *Nucleic Acids Res.* **45,** D1054–D1059 (2017).

18. Atwell, S. *et al.* Genome-wide association study of 107 phenotypes in Arabidopsis thaliana inbred lines. *Nature* **465,** 627–631 (2010).

19. Purcell, S. *et al.* PLINK: a tool set for whole-genome association and population-based linkage analyses. *Am. J. Hum. Genet.* **81,** 559–575 (2007).

20. Exposito-Alonso, M. *et al.* Genomic basis and evolutionary potential for extreme drought adaptation in Arabidopsis thaliana. *Nat Ecol Evol* **2,** 352–358 (2018).

21. Itseez. Open Source Computer Vision Library. (2015). Available at: https://github.com/itseez/opencv.

22. Coelho, L. P. Mahotas: Open source software for scriptable computer vision. *Journal of Open Research Software* **1,** e3 (2013).

23. Vasseur, F., Wang, G., Bresson, J., Schwab, R. & Weigel, D. Image-based methods for phenotyping growth dynamics and fitness in Arabidopsis thaliana. *bioRxiv* (2018).

24. Brachi, B. *et al.* Coselected genes determine adaptive variation in herbivore resistance throughout the native range of Arabidopsis thaliana. *Proceedings of the National Academy of Sciences* **112,** 4032–4037 (2015).

25. Roux, F., Gasquez, J. & Reboud, X. The dominance of the herbicide resistance cost in several Arabidopsis thaliana mutant lines. *Genetics* **166,** 449–460 (2004).